Clinical Neurophysiology 127 (2016) 2022–2030

Contents lists available at ScienceDirect

Clinical Neurophysiology

journal homepage: www.elsevier.com/locate/clinph

Ascending vestibular drive is asymmetrically distributed to the inferior oblique motoneuron pools in a subset of hemispheric stroke survivors

Derek M. Miller [a,c,*], James F. Baker [a,b], W. Zev Rymer [a,b,c]

[a] Interdepartmental Neurosciences Program, Northwestern University, Chicago, IL 60611, USA
[b] Department of Physiology, Feinberg School of Medicine, Northwestern University, Chicago, IL 60611, USA
[c] Sensory Motor Performance Program, Rehabilitation Institute of Chicago, Chicago, IL 60611, USA

ARTICLE INFO

Article history:
Accepted 26 January 2016
Available online 18 February 2016

Keywords:
Hemispheric stroke
Post-stroke spasticity
Otolith-ocular pathways
Human
Motoneuron
Ocular vestibular evoked myogenic potentials

HIGHLIGHTS

- Ocular vestibular evoked myogenic potentials (OVEMPs) were larger on the clinically affected than spared side in stroke patients with spasticity.
- The magnitude of the evoked response on the clinically affected side correlated with the severity of spasticity measured in the elbow flexors in a subset of subjects.
- This study provides evidence that the functions of the vestibular nuclei are broadly altered in post-stroke spasticity, extending to alterations in vestibuloocular outputs.

ABSTRACT

Objective: Aberrant vestibular nuclear function is proposed to be a principle driver of limb muscle spasticity after stroke. Although spasticity does not manifest in ocular muscles, we sought to determine whether altered cortical modulation of ascending vestibuloocular pathways post-stroke could impact the excitability of ocular motoneurons.
Methods: Nineteen chronic stroke survivors, aged 49–68 yrs. were enrolled. Vestibular evoked myogenic potentials (VEMPs) were recorded from the inferior oblique muscles of the eye using surface EMG electrodes. We assessed the impact of ascending otolith pathways on eye muscle activity and evaluated the relationship between otolith-ocular function and the severity of spasticity.
Results: VEMP responses were recorded bilaterally in 14/19 subjects. Response magnitude on the affected side was significantly larger than on the spared side. In a subset of subjects, there was a strong relationship between affected response amplitude and the severity of limb spasticity, as estimated using a standard clinical scale.
Conclusions: This study suggests that alterations in ascending vestibular drive to ocular motoneurons contribute to post-stroke spasticity in a subset of spastic stroke subjects. We speculate this imbalance is a consequence of the unilateral disruption of inhibitory corticobulbar projections to the vestibular nuclei.
Significance: This study potentially sheds light on the underlying mechanisms of post-stroke spasticity.

1. Introduction

Spasticity is a frequent and often disabling sequel to hemispheric stroke (Watkins et al., 2002; Urban et al., 2010; Wissel et al., 2013). It is characterized by a velocity-dependent increase in the resistance of a limb to passive stretch, coupled with exaggerated tendon jerks resulting from hyperexcitability of the segmental reflex arc (Dietz and Sinkjaer, 2007; Lance, 1980). The etiology of spasticity is complex, and while emerging evidence implicates changes in motoneuron excitability (*i.e.*, *decreased reflex threshold*; *spontaneous motoneuron firing at sub-threshold levels*) as central to the genesis of post-stroke spasticity (Chung et al., 2008; Mottram et al., 2009; Hu et al., 2015), the physiological drivers underlying

* Corresponding author at: University of Pittsburgh School of Medicine, Eye & Ear Institute Building, 203 Lothrop Street, Room 109, Pittsburgh, PA 15213, USA. Fax: +1 412 647 8018.
E-mail address: derekmiller@pitt.edu (D.M. Miller).

http://dx.doi.org/10.1016/j.clinph.2016.01.019
1388-2457/

hyperexcitability are incompletely understood (Katz and Rymer, 1989; Burke et al., 2013). This paucity of knowledge is due in part to the lack of a widely accepted animal model of hemispheric stroke (Wright and Rang, 1990; Sheean, 2001) and the multifactorial origins of the disorder (Dietz and Sinkjaer, 2007). Although there is an incomplete understanding of the pathophysiology of the enhanced motoneuron excitability, there are converging lines of evidence suggesting that there is an increase in excitatory synaptic input to limb motoneurons secondary to cerebral stroke.

Indirect evidence suggests that post-stroke changes in motoneuron excitability are due to a common low-level depolarizing drive impinging on the resting spastic–paretic motoneuron pool (Burke and Ashby, 1972; Burke et al., 1972; Burne et al., 2005; Mottram et al., 2009). We (and many others) have suggested that there is a stroke-mediated disruption of lateralized corticobulbar pathways that normally suppress vestibular nuclear activity (Burke et al., 1972; Burke and Ashby, 1972; Powers et al., 1988; Katz and Rymer, 1989; Burne et al., 2005; Mottram et al., 2009). The resulting release of excitatory brainstem pathways places spinal motoneurons in a hyperexcitable state (Katz and Rymer, 1989). Enhanced input from excitatory vestibulospinal pathways has long been implicated as one of the principal drivers of the increased spinal reflex activity characteristic of post-stroke spastic hypertonia (Denny-Brown, 1964, 1965; Burke, 1988; Katz and Rymer, 1989). In a recent study, we demonstrated that spasticity is likely a reflection of imbalanced vestibulospinal drive to limb motoneurons (Miller et al., 2014). Such disturbances are not limited to enhanced spinal and muscular reflex activity. Notable balance and postural deficits (Marsden et al., 2005), perceptual abnormalities (Baier et al., 2012), and aberrant oculomotor control (Dichgans et al., 1978; De Renzi et al., 1982; Tijssen et al., 1991; Catz et al., 1994; Singer et al., 2006) are commonly reported sequelae to hemispheric stroke that are associated with compromised vestibular function.

While spasticity does not occur in eye muscles, we were interested in determining whether altered cortical regulation of ascending vestibular pathways arises secondary to stroke in subjects presenting with spasticity, or if the asymmetries observed are unique to descending vestibular pathways. One standard test for evaluating ascending vestibular reflex function is the ocular vestibular evoked myogenic potential or OVEMP (Chihara et al., 2007; Todd et al., 2007; Welgampola et al., 2009; Curthoys, 2010). The OVEMP is a short-latency biphasic surface EMG potential reflecting the synchronous activation of inferior oblique motoneurons (Rosengren et al., 2005; Todd et al., 2007; Weber et al., 2012) presumptively mediated through the activation of crossed otolith-ocular pathways (Welgampola et al., 2009; Weber et al., 2012). The pathway mediating the response to air-conducted stimuli is widely believed to arise from irregularly firing afferents innervating the otoliths (McCue and Guinan, 1994; Curthoys et al., 2012), synapsing in the ipsilateral vestibular nucleus and ascending via the contralateral medial longitudinal fasciculus to synapse on the motoneurons of the inferior oblique (*i.e., crossed short latency otolith-ocular pathway*) (Weber et al., 2012) (Fig. 1a).

In the present study, we assessed the impact of ascending otolith-related pathways on eye muscle activity in hemiparetic stroke survivors and evaluated the relationship between otolith-ocular function and the severity of spasticity. Our central hypothesis is that a hemispheric lesion resulting in limb muscle spasticity leads to an imbalance in the activity of ascending vestibuloocular pathways (*due to shared anatomy*). In this scenario, a lateralized disruption in corticobulbar projections releases the spastic–paretic (*clinically affected*) vestibular nuclei and their associated ascending and descending pathways from inhibitory cortical control. We postulate that within an individual subject, the degree of asymmetry in OVEMP amplitude between the spastic–paretic and contralateral sides reflects an imbalance in ascending vestibuloocular drive. Accordingly, the objective of the current study was to examine the activation of inferior oblique motoneurons by ascending vestibular projections in the spastic stroke subject. To address this objective, the OVEMP reflex amplitude was used to estimate the relative levels of otolith-ocular drive to extraocular motoneuron pools. Additionally, to examine the relationship of ascending vestibular drive to the extraocular motor nuclei and limb spasticity, we compared the amplitude of the eye muscle reflex with the level of limb reflex activation.

2. Subjects and methods

The Northwestern University Institutional Review Board approved all experimental procedures. In accordance with the Declaration of Helsinki, all subjects gave informed written consent before experimentation. To differentiate between the clinically impaired (*spastic–paretic*) and spared (*unaffected*) sides, the vestibular nuclear complex and inferior oblique muscle located contralesionally will be classified as clinically affected (CA). In a similar manner, the vestibular nuclear complex and inferior oblique muscle located ipsilateral to the cortical lesion will be classified as clinically spared (CS).

2.1. Subjects

Nineteen chronic stroke survivors (12 males, 7 females; 138.0 ± 104.9 months post-stroke), ranging in age from 49 to 68 (58.6 ± 4.7 yrs.) participated in the study. Survivors had a single unilateral cortical or subcortical brain lesion resulting in spastic hemiparesis. A dedicated research physical therapist assessed spasticity at the elbow using the magnitude of the biceps tendon reflex (0–4) and the Modified Ashworth Scale (MAS), a 6-point rating scale used to measure passive muscle resistance (Bohannon and Smith, 1987). Functional recovery was assessed in the upper extremities using the 66-point upper extremities motor domain of the Fugl-Meyer Assessment (Fugl-Meyer et al., 1975). A Fugl-Meyer score of 0 indicates complete paresis of the limb, whereas a score of 66 indicates normal motor function. All subjects reported a negative history for vestibular, neurological, and auditory deficits. No subject was using vestibular suppressant medications. To exclude significant hearing loss, pure tone screening audiometry was performed at four frequencies (0.25, 0.5, 1 and 2 kHz) using the Modified Hughson-Westlake paradigm (Earscan 3 Manual Audiometer, Micro Audiometrics Corp., Murphy, North Carolina, USA). Subjects were excluded if they had greater than a 10 dB difference in hearing threshold between the left and right ears at 0.5 kHz. Table 1 details pertinent demographic and clinical information for each subject.

2.2. Methods

2.2.1. Surface recordings

EMG recording sites located on the forehead, cheeks, and infraorbital margins were prepared using an abrasive isopropyl alcohol pad and Nu-Prep Gel (Weaver and Company, Aurora, CO) prior to electrode placement. Surface electromyograms (EMG) were recorded from the inferior oblique muscles using single differential Delsys surface electrodes (Delsys Bagnoli-8 Channel EMG System, Delsys Inc., Natick, MA) placed in alignment with the pupil just inferior to the eye on the infra-orbital margin. Each Delsys surface sensor is a differential electrode housed in a polyurethane shell containing a preamplifier and two parallel silver

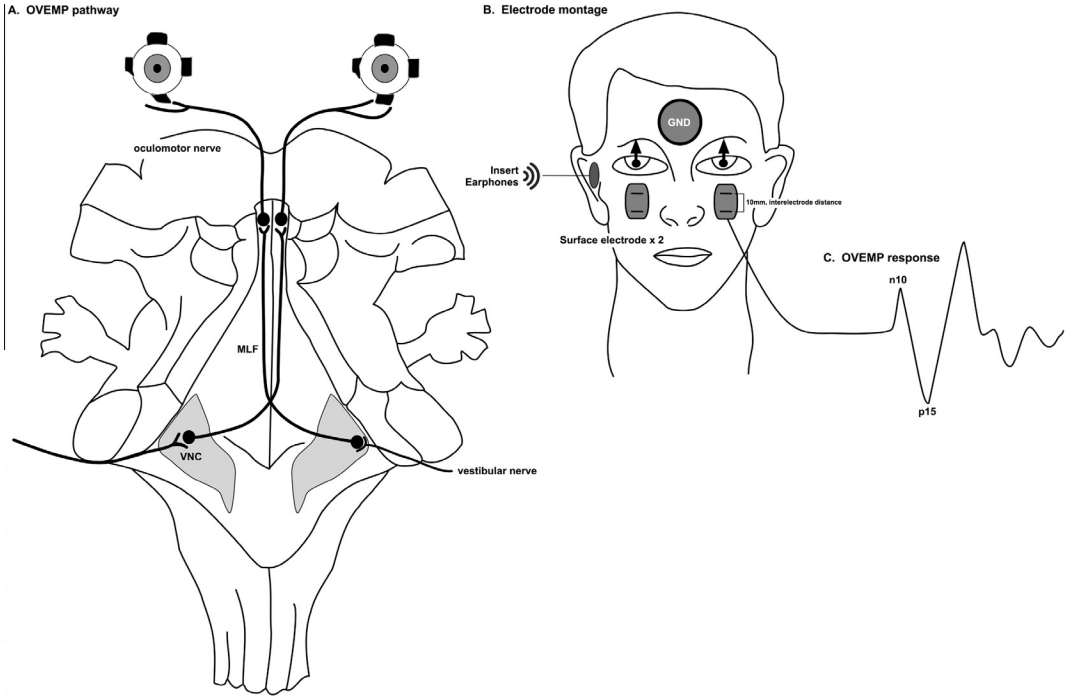

Fig. 1. A crossed otolith-ocular pathway is presumed to mediate the OVEMP. Figure modified and reproduced with permission from Elsevier, Rosengren et al. (2010). (a) The presumed OVEMP pathway consists of the primary afferents, vestibular nuclear complex (VNC), medial longitudinal fasciculus (MLF), oculomotor nuclei, and the corresponding nerves. (b) Electrode montage used to record OVEMPs from the inferior oblique muscles. (c) Representative stimulus trigger averaged unrectified OVEMP evoked in response to acoustic stimulation of the contralateral ear (i.e. stimulate right ear, measure left eye).

Table 1
Subject demographic and clinical information from 19 chronic stroke survivors.

Subject ID	Age, yrs.	Sex	Months post stroke	MAS elbow flexors	UEFM	Lesion location	Paretic side/hand dominance
Responses present on both sides (N = 14)							
1	59	M	125	1	50	L IC and CR	R/L
4	49	M	53	1	40	R IC	L/R
6	64	M	258	3	13	L MCA	R/R
7	59	M	69	3	11	R CR, posterior limb IC and lentiform nucleus	L/R
8	66	F	57	3	7	R MCA and BG	L/R
9	57	M	38	1	54	L BG	R/R
10	55	M	66	2	22	Left thalamic hemorrhage (midline shift)	R/L
11	58	M	102	3	19	L lateral thalamic and BG	R/R
13	56	F	117	3	19	R BG hemorrhage	L/R
14	68	M	235	2	8	L temporal and parietal lobes	R/L
15	58	M	87	1+	18	R basal ganglia PPR	L/R
17	62	F	320	2	22	L internal carotid artery dissection PPR	R/R
19	55	M	80	1	17	R IC, MCA and frontotemporal insular cortex	L/L
21	61	F	336	1+	11	L BG and IC	R/R
Unilateral responses, spastic-paretic or non-paretic (N = 3)							
3	58	M	310	2	20	U	L/R
16	63	F	34	3	4	R BG hemorrhage PPR	L/R
20	52	F	47	1	10	L BG hemorrhage	R/L
Absent responses, both sides (N = 2)							
2	55	F	68	1	50	L MCA	R/R
18	58	M	220	0	12	U	L/R

Neuroanatomical abbreviations: BG, basal ganglia; CR, corona radiata; IC, internal capsule; MCA, middle cerebral artery; U, unknown; PPR, per patient report.
Clinical measurements: MAS, Modified Ashworth Score; UEFM, Upper Extremity Fugl Meyer (UE maximum score = 66).

contact bars (10 mm L × 1 mm W) with a 10-mm fixed inter-electrode distance. A single adhesive ground electrode was placed high on the forehead (Dermatrode Reference Electrode, American Imex, Irvine, CA). EMG signals were amplified by a factor of 100 K, band-pass filtered 0.02–0.45 kHz, and sampled at 10 kHz. Fig. 1b provides an illustration of the electrode montage used to record the OVEMP response.

2.2.2. Experimental protocol

Experiments were conducted in a quiet, dimly lit room. Subjects lay supine on an examination table, with their head placed in a cradle that served to support the cervical spine and minimize lateral head rotation. Each subject was instructed to fixate on a small target located 97 cm behind and 165 cm above their head that served to elevate the eyes approximately 25–30° relative to the visual

straight ahead causing contraction of the inferior oblique muscle. This position is required to record a VEMP (Rosengren et al., 2005; Govender et al., 2009). Acoustic stimuli were generated using the Biologic Navigator Pro Auditory Evoked Potential system (NavPro AEP System, Natus Medical, San Carlos, CA). The sound stimulus was a 500 Hz air-conducted short tone burst, presented at a rate of 5 per second with rarefaction polarity and Blackman ramping (2 cycles plateau and 1 cycle rise and fall times). Each trial consisted of two trains of sixty-four short tone bursts delivered monaurally via foam E-A-R Tone 3A insert earphones (E-A-R Auditory Systems, Indianapolis, IN) with an impulse intensity of 95 dB nHL (130 dB SPL) while the subject fixated on the target. At least two trials were obtained from each side in response to stimulation of the contralateral ear (*i.e.*, *stimulate left ear*, *record right inferior oblique*). For each side, two trials were averaged together to generate the final response. Subjects were given 30–45 s rest periods between trains and rest periods of 2–4 min between trials to reduce eyestrain. Testing occurred in one session lasting approximately 180 min. Head and eye position were regularly checked to ensure consistency. A sham trial consisting of no sound stimulation was randomly presented to confirm that responses were not due to inherent variability in the signal or to signal processing methods.

2.2.3. Waveform analysis

For each trial, the unrectified EMG was stimulus-triggered averaged to acoustic tones over an epoch of 70 ms (20 ms prior to stimulus onset – 50 ms post-stimulus onset) using a Power 1401 analog to digital converter coupled with a PC running Spike 2 software (Cambridge Electronic Design, Cambridge, UK). Waveform averages were analyzed offline using customized software programs (Spike 2, Cambridge Electrode Design, Cambridge, UK; Matlab, Mathworks Inc., Natick, MA) for peak amplitude and onset latency. We defined the OVEMP as a reproducible biphasic potential with an interpeak amplitude that exceeded a two standard deviation bandwidth, calculated from the unrectified prestimulus baseline average over a 20 ms period. Responses exceeding this band were considered significant and were included for further analysis. Peak latencies were measured from the unrectified stimulus-triggered waveform average, calculated with respect to stimulus onset, and were defined as n10 and p15 (Fig. 1c). A peak was labeled n10 if it occurred between 10 and 20 ms post-stimulus onset and exceeded the two standard deviation band. The subsequent peak of opposite polarity immediately following n10 was designated as p15. The interpeak amplitude (n10–p15) was calculated by summing the absolute magnitude of the n10 and p15 peaks, and the interpeak interval was calculated by subtracting the n10 onset latency from the p15 onset latency. Side-to-side differences in OVEMP response amplitudes were quantified by expressing the CA and CS interpeak amplitudes as an asymmetry ratio (AR,%), an analog used to represent the relative amount of otolith-ocular drive impinging on each motoneuron pool. The asymmetry ratio was defined as $100 \times ((\text{CA interpeak amplitude} - \text{CS interpeak amplitude}) \div (\text{CA interpeak amplitude} + \text{CS interpeak amplitude}))$. It was necessary to edit out the occasional blink, as the amplitude of the OVEMP is small relative to the EMG activity generated by blinking (range: 116–128 per trial).

2.2.4. Statistical analysis

Data are expressed in terms of mean ± standard deviation unless otherwise noted. Statistical analysis was performed using Prism 6 (Graph Pad Software, Inc., La Jolla, CA). The interpeak amplitudes, peak onset latencies (n10, p15), and interpeak intervals from each subject were averaged to calculate the respective CA and CS population means. For statistical comparisons of numerical data, we used a non-parametric Wilcoxon matched-pairs signed rank test or a paired *t*-test according to the normality distribution of the data. A Wilcoxon matched-pairs signed rank test was used to compare the CA and CS interpeak amplitude values, which were first log transformed because of an extreme outlier (subj. 8). Correlations are expressed as a nonparametric Spearman's rank coefficient. For all statistical comparisons, a p-value $\leqslant 0.05$ was considered to be significant.

3. Results

OVEMPs were observed bilaterally, on both the CA and CS sides, in 14/19 subjects (74%). Observed responses were similar in latency and morphology to those previously reported in healthy control subjects (Rosengren et al., 2011). Three subjects had unilaterally absent responses (3/19 subjects, 16%), and the remaining two subjects had absent responses bilaterally (2/19 subjects, 10%). Two of the three subjects presenting with unilaterally absent responses had a basal ganglia hemorrhage. It is conceivable that a diffuse lesion involving multiple cortical and subcortical areas, as would potentially occur following a hemorrhagic stroke, would affect ascending and descending pathways involved with oculomotor control. It is known that several oculomotor pathways traverse the internal capsule (Morrow and Sharpe, 1990), and damage to these pathways could result in absent OVEMPs. While it is not possible to determine the origins of the absent or unilateral responses, for this study only subjects with responses present on both sides were included in the statistical analysis.

3.1. Amplitude

OVEMPs elicited on the CA and CS sides from the 14 subjects with bilateral responses are superimposed and depicted in Fig. 2. The mean interpeak amplitude on the CA side was 0.77 ± 0.59 μV (range [0.27, 2.6]; 95% CI [0.43, 1.1]) and 0.57 ± 0.33 μV (range

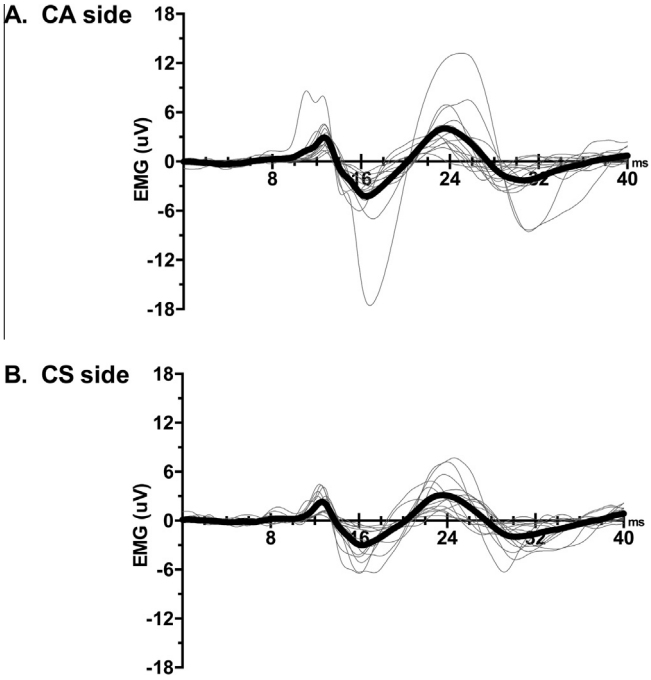

Fig. 2. Individual OVEMPs (*thin lines*) obtained from the clinically affected (a) and clinically spared (b) inferior oblique muscles contralateral to stimulation in 14 chronic stroke survivors. Each thin trace represents the average of two trials. The clinically affected and clinically spared population responses (n = 14 subjects; **bold line**) are superimposed on the appropriate subplot.

[0.14, 1.1]; 95% CI [0.38, 0.76]) on the CS side. To allow for a comparison of the means, the data was log transformed. When compared, the population CA interpeak amplitude (*log transformed*) was significantly larger than the population CS interpeak amplitude (*log transformed*) ($n = 14$ subjects; Wilcoxon matched-pairs signed rank test; p-value = 0.0245, Fig. 3).

Across subjects, asymmetry ratios (%) were widely distributed ranging from −25 to 41. Based on the findings of a previous study (Miller et al., 2014), subjects were broken into two groups contingent on the polarity of the asymmetry ratio. Four subjects (4/14 subjects, 29%) had negative asymmetry ratios (termed AR^{neg}) indicating that the interpeak amplitude was smaller on the CS side when compared to the CA side. The mean asymmetry ratio for AR^{neg} subjects was −10 ± 11%, ranging from −25% to −0.49% (95% CI [−26, 8]). The remaining ten subjects (10/14 subjects, 71%) had positive asymmetry ratios (AR^{pos}, Fig. 4). The mean asymmetry ratio for AR^{pos} subjects was 24 ± 13%, ranging from 2% to 41% (95% CI [15, 33]). To evaluate the relationship between the magnitude of the OVEMP elicited on the CA side and the degree of spasticity in AR^{pos} subjects, we plotted the individual CA interpeak amplitudes from the 10 AR^{pos} subjects as a function of the MAS measured in the elbow flexor muscles ($n = 10$ subjects; Spearman $r = 0.71$; p-value = 0.0278; Fig. 5). There was a modest correlation between the asymmetry ratio and the severity of spasticity in AR^{pos} subjects; however, the relationship was not significant ($n = 10$ subjects; Spearman $r = 0.48$; p-value = 0.1578; Fig. 6).

3.2. Response latencies

There were no statistically significant differences in $n10$ peak latencies between the two sides ($n = 14$ subjects; Wilcoxon matched-pairs signed rank test; p-value = 0.9983). The mean CA and CS n10 peak latencies were 12.7 ± 0.55 ms (range [11.1, 13.3]; 95% CI [12.3, 13.0]) and 12.7 ± 0.29 ms (range [12.2, 13.2]; 95% CI [12.5, 12.9]) respectively. The CS p15 peak latency was significantly prolonged when compared to the CA side ($n = 14$ subjects; Wilcoxon matched-pairs signed rank test p-value = 0.0026). The mean CA p15 onset latency was 16.4 ± 0.70 ms (range [14.6, 17.2]; 95% CI [16.0, 16.8]) and 16.9 ± 0.74 ms (range [16.0, 18.4]; 95% CI [16.4, 17.3]) on the CS side. Additionally, the CA mean interpeak interval at 3.7 ± 0.82 ms (range [1.9, 5.7]; 95% CI [3.2, 4.2]) was significantly shorter ($n = 14$ subjects; Paired t-test, p-value = 0.0257) in duration than the CS mean interpeak interval, 4.2 ± 0.74 ms (range [3.2, 5.6]; 95% CI [3.7, 4.6]).

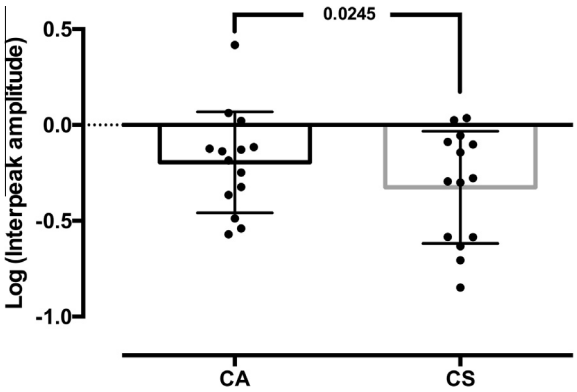

Fig. 3. Histogram displaying population averaged CA and CS interpeak amplitudes (*log transformed*) from 14 subjects that had responses bilaterally. Each filled circle represents the CA or CS interpeak amplitude from a subject. Population means were compared using a Wilcoxon matched-pairs signed rank test. Mean and standard deviation are plotted.

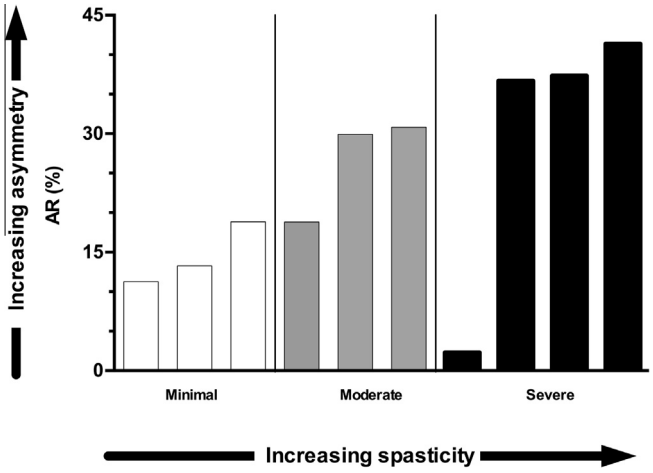

Fig. 4. AR positive subjects were binned according to the severity of spasticity measured in the elbow flexors. Within each bin, subjects were rank-ordered in terms of increasing AR.

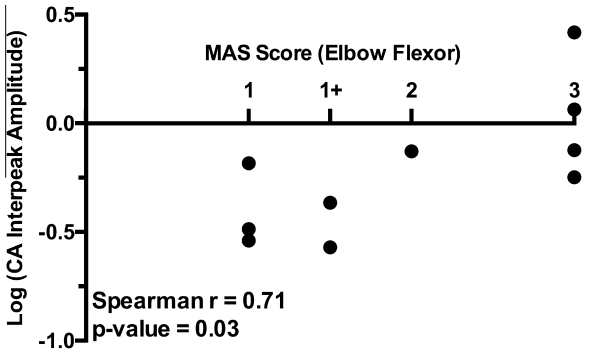

Fig. 5. For the AR^{pos} subjects, a significant correlation existed between the magnitude of the log transformed CA interpeak amplitude and the severity of spasticity measured in the elbow flexors. The Spearman correlation coefficient and p-value are indicated in the lower left of the figure.

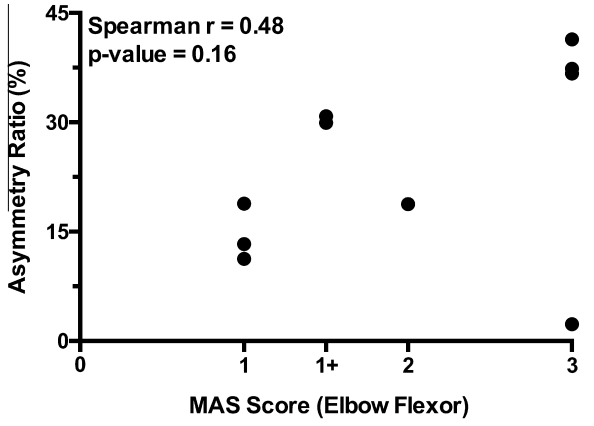

Fig. 6. A modest correlation between the asymmetry ratio and the severity of spasticity in AR positive subjects exists, however the relationship was not significant. The Spearman correlation coefficient and p-value are indicated in the upper left of the figure.

4. Discussion

The present study examined the relative distribution of otolith-ocular drive to the clinically affected and spared inferior oblique muscles in chronic hemiparetic stroke survivors presenting with

spasticity of cerebral origin. We characterized the relationship between the magnitude of the CA response and the severity of spasticity. In the majority of subjects (10/14 subjects), the OVEMP on the CA side was larger in amplitude when compared to the CS side, an effect reversed in four subjects. Furthermore, in AR^{pos} subjects we found a significant relationship between the magnitude of the CA interpeak amplitude and the severity of limb spasticity. These data extend our previous observations showing that vestibular drive to cervical motoneurons is asymmetrically distributed in a subset of spastic stroke survivors and that these side-to-side differences in OVEMP amplitude scaled with the clinically assessed severity of spasticity (Miller et al., 2014). Our results lend support to the notion that there is an imbalance in vestibular drive to motoneuron pools post-stroke, however, additional future studies are warranted.

4.1. Quantification of vestibular drive

Human extraocular musculature is richly endowed with muscle spindles that are morphologically distinct from their skeletal muscle counterparts (Wicke et al., 2007). Recordings made from extraocular spindle afferent fibers show that unlike skeletal muscle spindle afferents, extraocular spindle afferents do not respond well to muscle stretch (Keller and Robinson, 1971). Additionally, there is no closed loop connection back to the extraocular motoneuron. Consequently, human extraocular muscles lack a neurally mediated stretch reflex. For this reason, spasticity cannot arise in extraocular musculature because there are no stretch reflexes available to be augmented. We suggest that the interpeak amplitude and asymmetry ratio can be used as proxies' indicative of the relative degree of vestibular input impinging upon the CA and CS inferior oblique motoneuron pools, rather than a direct measure of motoneuron excitability. This assumption is chiefly based on a study drawn from the biceps brachii of stroke survivors, in which side-to-side differences in reflex amplitude disappear when background EMG levels are matched (Burne et al., 2005). Moreover, given that eye elevation was fixed and barring changes in the biomechanics of the extraocular plant or systematic alterations in peripheral vestibular afferent input, differences in interpeak amplitude between the CA and CS sides could thus be attributed to the amount of vestibular drive impinging upon each motoneuron pool. It follows that as the magnitude of the OVEMP interpeak amplitude likely depends on the extent of damage to the corticobulbar fibers, we expect that there would be a correlation between the CA interpeak amplitude and the severity of spasticity in AR^{pos} subjects.

While the majority of subjects had positive asymmetry ratios, four had consistently larger responses on their CS side. The discordance in asymmetry ratio polarity is not unexpected, due in part to inherent intersubject variability arising as a consequence of the considerable variation in factors such as the site and size of the lesion, as well as the time post-stroke (Teasell et al., 2005). All subjects were recruited and screened by a dedicated research physical therapist using strict inclusion and exclusion criteria to mitigate the impact of these variables on the subject pool. It is conceivable that diffuse vascular lesions, which typically involve multiple cortical and subcortical areas would likely impact ascending pathways routed through the internal capsule involved with oculomotor control (Morrow and Sharpe, 1990). Collateral damage to these pathways could result in asymmetric oculomotor function that would not be due to aberrant vestibular function. However, abnormalities caused by the disruption of the inferior parietal lobule and frontal eye field associated pathways typically accompanies spatial neglect (Fruhmann Berger et al., 2006), which was not manifested in any of our subjects. Alternatively, it is possible that the MAS measurements may not have accurately reflected spinal reflex excitability. The MAS is confounded by potential concurrent muscle contracture (Patrick and Ada, 2006), a scenario where the increased mechanical resistance is due to peripheral changes in muscle properties rather than to changes in stretch reflex excitability (O'Dwyer et al., 1996). AR^{neg} subjects were at least 38 months' post-stroke (mean 165.5 ± 134.5; range: 38–320 months' post-stroke) allowing ample time for soft-tissue changes and muscle contracture to set in. Furthermore, quantification of the deep tendon reflexes, a measure of phasic reflex excitability, indicated that these subjects tended to have normal to hypoactive reflexes in the biceps and triceps.

4.2. Potential neural mechanisms for spasticity

Sherrington (1898) provided indirect evidence demonstrating the inhibitory nature of corticobulbar projections. Immediately following the removal of all cortical input to the brainstem, there is an exaggeration of postural reflexes characterized by increased extensor tone in all extremities that appears to be driven by unopposed supraspinal drive to the antigravity motoneuron pools (Bach and Magoun, 1947; Fulton and Liddell, 1930). Selective lesioning of brainstem motor nuclei alleviates the effect of the tonic supraspinal drive on muscle tone. Although decerebration is not a precise analog for human stroke, the loss of cortical modulation following the removal of corticobulbar input parallels many of the clinical observations seen following hemispheric stroke in humans. The loss of cortical control over brainstem output appears to arise following the disinhibition of brainstem nuclei (Magoun and Rhines, 1946) and the release of descending bulbospinal drive that exerts powerful control over the excitability of the segmental reflex arc (Young, 1994; Burke et al., 2013).

4.2.1. Imbalanced supraspinal drive

Detailed retrograde-tracing studies in non-human primates reveal cortical projections linking the parietal insular vestibular cortex and premotor areas to the ipsilateral rostral medial and superior vestibular nuclei (Akbarian et al., 1993, 1994). These nuclei have strong projections to oculomotor centers (Mitsacos et al., 1983; Carpenter and Cowie, 1985). These cortical projecting fibers are believed to play a dominant role in gaze stabilization through the suppression of vestibular motor reflex arcs during goal-directed movements (Akbarian et al., 1994). Based on these anatomical data, we speculate that a lesion disrupting corticobulbar projections from the left (*or right*) hemisphere would disinhibit the ipsilesional rostral medial and superior vestibular nuclei. Given the crossed trajectory of the otolith-ocular pathways (Welgampola et al., 2009; Weber et al., 2012), we would expect to see increased drive to the right or contralesionally located inferior oblique relative to the left ipsilesionally located inferior oblique.

The anatomy underlying corticovestibular projections is compatible with the sharply lateralized manifestation of spasticity on the side opposite the cerebral lesion. Specifically, premotor areas send direct projections to the contralateral caudal medial and lateral vestibular nuclei (Akbarian et al., 1993, 1994) that influence contralateral spinal reflex circuitry through the sharply lateralized vestibulospinal projection neurons. Therefore, in addition to the oculomotor effects, the lesion theoretically disinhibits the right caudal medial and lateral vestibular nuclei, which influence right-sided motoneuron excitability. While an asymmetry in vestibular nuclear outflow to the clinically affected and clinically spared motoneuron pools is the most parsimonious explanation for our findings, other explanations are certainly conceivable.

Prior research shows a lateralized increased startle reflex amplitude in about 25% of stroke subjects (Jankelowitz and Colebatch, 2004). The classic auditory start reflex, a subcortical reflex that arises following sudden and intense acoustic stimulation, is

mediated by reticulospinal pathways that arise in the nucleus reticular gigantocellularis and nuclear reticularis pontis caudalis (Wilson and Peterson, 2011). Cortical involvement is questioned, due in part to the bilateral distribution of corticoreticular projections (Matsuyama and Drew, 1997; Rho et al., 1997) and the finding that spinal cord injured patients also exhibited increased startle, which indicates a possible change at the segmental level (Jankelowitz and Colebatch, 2004). Additionally, reticulospinal pathways cannot easily explain the sharply lateralized nature of spasticity. Reticulospinal pathways are bilaterally organized in both their anatomical spinal distribution (Nyberg-Hansen, 1965; Nathan et al., 1996; Jankowska et al., 2003; Schepens and Drew, 2006; Davidson et al., 2007) and synaptic action (Matsuyama and Drew, 1997; Rho et al., 1997; Davidson and Buford, 2006; Davidson et al., 2007; Schepens and Drew, 2006). However, we cannot entirely dismiss reticular pathways given the extensive interconnection of the vestibular and the reticular complexes (Ladpli and Brodal, 1968; Carleton and Carpenter, 1983).

4.2.2. Abnormal intraspinal processing of afferent input

There are other possible mechanisms that could explain the asymmetrical response type. It is possible that the alpha motoneuron itself becomes intrinsically more excitable through changes in the biophysical properties of the cell membrane following the stroke-mediated release of brainstem monoaminergic pathways (Katz and Rymer, 1989). The augmentation of monoaminergic drive to the spinal cord could lead to an enhancement of persistent inward currents (PICs), which are slowly inactivating voltage-sensitive Na^+ and Ca^{2+} currents subjected to strong neuromodulation by serotonin and norepinephrine (Hounsgaard et al., 1988). PIC activation could lead to the development of plateau potentials (*self-sustained firing*) or increase the likelihood of motoneuron discharge through amplification of muscle spindle afferent or other sensory input (*gain* ↑) (Lee and Heckman, 2000; Li et al., 2004; Heckmann et al., 2005). While there is evidence for the role of PICs in spinal forms of spasticity (Barbeau et al., 1981; Li et al., 2004), there is meager evidence to support a role for enhanced PICs and monoamines in cerebral forms of spasticity (Mottram et al., 2009). Furthermore, monoaminergic projections originating in the brainstem are diffuse and bilateral (Björklund and Skagerberg, 1982), making them incompatible with the sharply lateralized nature of stroke-induced spasticity. Alternatively, increased sensitivity of group Ia primary and group II secondary muscle spindle afferents to stretch due to enhancement of gamma fusimotor drive could contribute to our findings through an increase in the gain of the stretch reflex. While there is no evidence for a post-stroke enhancement of spindle afferent sensitivity (Wilson et al., 1999) to date, there is evidence for a reduction in presynaptic inhibition (Lamy et al., 2009) although this is bilaterally distributed within the spinal cord and correlates poorly with the severity of spasticity. Finally, changes in spinal reflex circuitry may occur following stroke, such as a facilitation of group Ib and II afferents or a reduction in reciprocal inhibition, but as Burke et al. (2013) noted, current research has yielded conflicting results that often correlate poorly with spasticity.

4.3. Limitations

We designated the clinically spared side as the control side in the current study. However, it is possible that the clinically spared side is also affected by the stroke, even in the absence of overt clinical impairment or symptomatology. Nonetheless, within-subject comparisons (i.e. *between sides*) are preferable to comparisons against normal aged-matched control subjects because of the large between-subject variability (Hu et al., 2015) in OVEMP amplitude (Figs. 2 and 3) and subject characteristics (i.e., *time post-stroke, lesion location, clinical scores*).

4.4. Future directions

This study provides evidence for an asymmetric distribution of otolith drive to the CA and CS motoneuron pools post-stroke however, these findings are solely correlative, and further studies are needed to investigate a causal role for these putative otolith-ocular pathways. While we chose to investigate otolith-ocular pathways, because of the postulated role of descending otolith pathways in the genesis and maintenance of post-stroke spasticity, it is likely that canal mediated reflexes are also disinhibited.

The importance of hemispheric influences on the modulation of the canal mediated vestibuloocular reflex (VOR) is demonstrated in human subjects following hemidecortication, whereby there is an asymmetry in the voluntary modulation of the VOR in darkness (Estanol et al., 1980; Sharpe and Lo, 1981), presumably due to the unilateral loss of corticobulbar pathways. Indeed, following hemispheric stroke (Catz et al., 1994), there are permanent deficits in dynamic processes such as VOR gain modulation and VOR suppression, especially during sudden movements. This asymmetry is postulated to be due to a loss of cortical modulation of ascending vestibular nuclear activity (Catz et al., 1994; Dichgans et al., 1978). Collectively, these findings suggest that a disruption in the corticobulbar modulation of vestibular nuclear activity contributes to ocular deficits post-stroke. Investigation of these pathways warrants further research, especially given the availability of the video head impulse test (vHIT) which can be used for examination of the high-frequency canal-ocular reflex.

5. Conclusions

Several distinct elements influence muscle tone, including the intrinsic biomechanical properties of muscle and associated connective tissues, and active neurally mediated reflex mechanisms. Therefore, it is likely that the origins of the increased resistance to passive stretch as seen in the spastic stroke survivor are complex and multifactorial, depending on both alterations in the passive mechanical-elastic properties of the muscle and on impaired neurally mediated reflex activity (Chung et al., 2008). Our current observations provide evidence for an imbalance in otolith-ocular drive following a hemispheric stroke resulting in spasticity. The moderate correlation between CA interpeak amplitude with spasticity severity may indicate a relationship between the size of the corticobulbar lesion and the amount of disinhibition in the vestibular nuclei. Larger cortical or subcortical lesions likely disrupt more corticobulbar fibers, resulting in greater disinhibition of second order vestibular neurons and their associated pathways. We conclude that in a subset of hemispheric stroke survivors, oculomotor dysfunction potentially constitutes a release phenomenon; similar in nature to the spasticity seen in the antigravity musculature, whereby disinhibited otolith-ocular pathways drive extraocular motoneuron activity potentially leading to oculomotor deficits.

Acknowledgments

This work was supported by an American Heart Association Predoctoral Fellowship (Miller, 12PRE11840025). Derek M. Miller is now affiliated with the Department of Otolaryngology, University of Pittsburgh, Pittsburgh, Pennsylvania, 15213.

Conflict of interest: None of the authors have potential conflicts of interest to be disclosed.

References

Akbarian S, Grusser OJ, Guldin WO. Corticofugal projections to the vestibular nuclei in squirrel monkeys: further evidence of multiple cortical vestibular fields. J Comp Neurol 1993;332:89–104.

Akbarian S, Grusser OJ, Guldin WO. Corticofugal connections between the cerebral cortex and brainstem vestibular nuclei in the macaque monkey. J Comp Neurol 1994;339:421–37.

Bach LM, Magoun HW. The vestibular nuclei as an excitatory mechanism for the cord. J Neurophysiol 1947;10:331–7.

Baier B, Suchan J, Karnath HO, Dieterich M. Neural correlates of disturbed perception of verticality. Neurology 2012;78:728–35.

Barbeau H, Filion M, Bedard P. Effects of agonists and antagonists of serotonin on spontaneous hindlimb EMG activity in chronic spinal rats. Neuropharmacology 1981;20:99–107.

Björklund A, Skagerberg G. Descending monoaminergic projections to the spinal cord. In: Sjolund B, Björklund A, editors. Brain stem control of spinal mechanisms. Amsterdam: Elsevier Biomedical Press; 1982. p. 55–88.

Bohannon RW, Smith MB. Interrater reliability of a modified Ashworth scale of muscle spasticity. Phys Ther 1987;67:206–7.

Burke D. Spasticity as an adaptation to pyramidal tract injury. Adv Neurol 1988;47:401–23.

Burke D, Ashby P. Are spinal "presynaptic" inhibitory mechanisms suppressed in spasticity? J Neurol Sci 1972;15:321–6.

Burke D, Andrews CJ, Lance JW. Tonic vibration reflex in spasticity, Parkinson's disease, and normal subjects. J Neurol Neurosurg Psychiatry 1972;35:477–86.

Burke D, Wissel J, Donnan GA. Pathophysiology of spasticity in stroke. Neurology 2013;80:S20–26.

Burne JA, Carleton VL, O'Dwyer NJ. The spasticity paradox: movement disorder or disorder of resting limbs? J Neurol Neurosurg Psychiatry 2005;76:47–54.

Carleton SC, Carpenter MB. Afferent and efferent connections of the medial, inferior and lateral vestibular nuclei in the cat and monkey. Brain Res 1983;278:29–51.

Carpenter MB, Cowie RJ. Connections and oculomotor projections of the superior vestibular nucleus and cell group 'y'. Brain Res 1985;336:265–87.

Catz A, Ron S, Solzi P, Korczyn AD. The vestibulo-ocular reflex and dysequilibrium after hemispheric stroke. Am J Phys Med Rehabil 1994;73:36–9.

Chihara Y, Iwasaki S, Ushio M, Murofushi T. Vestibular-evoked extraocular potentials by air-conducted sound: another clinical test for vestibular function. Clin Neurophysiol 2007;118:2745–51.

Chung SG, van Rey E, Bai Z, Rymer WZ, Roth EJ, Zhang LQ. Separate quantification of reflex and nonreflex components of spastic hypertonia in chronic hemiparesis. Arch Phys Med Rehabil 2008;89:700–10.

Curthoys IS. A critical review of the neurophysiological evidence underlying clinical vestibular testing using sound, vibration and galvanic stimuli. Clin Neurophysiol 2010;121:132–44.

Curthoys IS, Vulovic V, Sokolic L, Pogson J, Burgess AM. Irregular primary otolith afferents from the guinea pig utricular and saccular maculae respond to both bone conducted vibration and to air conducted sound. Brain Res Bull 2012;89:16–21.

Davidson AG, Buford JA. Bilateral actions of the reticulospinal tract on arm and shoulder muscles in the monkey: stimulus triggered averaging. Exp Brain Res 2006;173:25–39.

Davidson AG, Schieber MH, Buford JA. Bilateral spike-triggered average effects in arm and shoulder muscles from the monkey pontomedullary reticular formation. J Neurosci 2007;27:8053–8.

De Renzi E, Colombo A, Faglioni P, Gibertoni M. Conjugate gaze paresis in stroke patients with unilateral damage. An unexpected instance of hemispheric asymmetry. Arch Neurol 1982;39:482–6.

Denny-Brown D. The extrapyramidal system and postural mechanisms. Clin Pharmacol Ther 1964;5:812–27.

Denny-Brown D. The Nature of dystonia. Bull N Y Acad Med 1965;41:858–69.

Dichgans J, Reutern GM, Rommelt U. Impaired suppression of vestibular nystagmus by fixation in cerebellar and noncerebellar patients. Arch Psychiatr Nervenkr 1978;226:183–99.

Dietz V, Sinkjaer T. Spastic movement disorder: impaired reflex function and altered muscle mechanics. Lancet Neurol 2007;6:725–33.

Estanol B, Romero R, Saenz de Viteri M, Mateos JH, Corvera J. Oculomotor and oculovestibular functions in a hemispherectomy patient. Arch Neurol 1980;37:365–8.

Fruhmann Berger M, Pross RD, Ilg U, Karnath HO. Deviation of eyes and head in acute cerebral stroke. BMC Neurol 2006;6:23.

Fugl-Meyer AR, Jaasko L, Leyman I, Olsson S, Steglind S. The post-stroke hemiplegic patient. 1. A method for evaluation of physical performance. Scand J Rehabil Med 1975;7:13–31.

Fulton JF, Liddell EGT, Mck. Rioch D. The influence of unilateral destruction of the vestibular nuclei upon posture and the knee jerk. Brain 1930;53:327–43.

Govender S, Rosengren SM, Colebatch JG. The effect of gaze direction on the ocular vestibular evoked myogenic potential produced by air-conducted sound. Clin Neurophysiol 2009;20:1386–91.

Heckmann CJ, Gorassini MA, Bennett DJ. Persistent inward currents in motoneuron dendrites: implications for motor output. Muscle Nerve 2005;31:135–56.

Hounsgaard J, Hultborn H, Jespersen B, Kiehn O. Bistability of alpha-motoneurones in the decerebrate cat and in the acute spinal cat after intravenous 5-hydroxytryptophan. J Physiol 1988;405:345–67.

Hu X, Suresh NL, Chardon MK, Rymer WZ. Contributions of motoneuron hyperexcitability to clinical spasticity in hemispheric stroke survivors. Clin Neurophysiol 2015;126:1599–606.

Jankelowitz SK, Colebatch JG. The acoustic startle reflex in ischemic stroke. Neurology 2004;62:114–6.

Jankowska E, Hammar I, Slawinska U, Maleszak K, Edgley SA. Neuronal basis of crossed actions from the reticular formation on feline hindlimb motoneurons. J Neurosci 2003;23:1867–78.

Katz RT, Rymer WZ. Spastic hypertonia: mechanisms and measurement. Arch Phys Med Rehabil 1989;70:144–55.

Keller EL, Robinson DA. Absence of a stretch reflex in extraocular muscles of the monkey. J Neurophysiol 1971;34:908–19.

Ladpli R, Brodal A. Experimental studies of commissural and reticular formation projections from the vestibular nuclei in the cat. Brain Res 1968;8:65–96.

Lamy JC, Wargon I, Mazevet D, Ghanim Z, Pradat-Diehl P, Katz R. Impaired efficacy of spinal presynaptic mechanisms in spastic stroke patients. Brain 2009;132:734–48.

Lance JW. Symposium synopsis. In: Feldman RG, Young RR, Koella WP, editors. Spasticity: disordered control. Chicago: Yearbook Medical; 1980. p. 485–94.

Lee RH, Heckman CJ. Adjustable amplification of synaptic input in the dendrites of spinal motoneurons in vivo. J Neurosci 2000;20:6734–40.

Li Y, Harvey PJ, Li X, Bennett DJ. Spastic long-lasting reflexes of the chronic spinal rat studied in vitro. J Neurophysiol 2004;91:2236–46.

Magoun HW, Rhines R. An inhibitory mechanism in the bulbar reticular formation. J Neurophysiol 1946;9:165–71.

Marsden JF, Playford DE, Day BL. The vestibular control of balance after stroke. J Neurol Neurosurg Psychiatry 2005;76:670–8.

Matsuyama K, Drew T. Organization of the projections from the pericruciate cortex to the pontomedullary brainstem of the cat: a study using the anterograde tracer Phaseolus vulgaris-leucoagglutinin. J Comp Neurol 1997;389:617–41.

McCue MP, Guinan Jr JJ. Acoustically responsive fibers in the vestibular nerve of the cat. J Neurosci 1994;14:6058–70.

Miller DM, Klein CS, Suresh NL, Rymer WZ. Asymmetries in vestibular evoked myogenic potentials in chronic stroke survivors with spastic hypertonia: evidence for a vestibulospinal role. Clin Neurophysiol 2014;125:2070–8.

Mitsacos A, Reisine H, Highstein SM. The superior vestibular nucleus: an intracellular HRP study in the cat. I. Vestibulo-ocular neurons. J Comp Neurol 1983;215:78–91.

Morrow MJ, Sharpe JA. Cerebral hemispheric localization of smooth pursuit asymmetry. Neurology 1990;40:284–92.

Mottram CJ, Suresh NL, Heckman CJ, Gorassini MA, Rymer WZ. Origins of abnormal excitability in biceps brachii motoneurons of spastic–paretic stroke survivors. J Neurophysiol 2009;102:2026–38.

Nathan PW, Smith M, Deacon P. Vestibulospinal, reticulospinal and descending propriospinal nerve fibres in man. Brain 1996;119:1809–33.

Nyberg-Hansen R. Sites and mode of termination of reticulo-spinal fibers in the cat. An experimental study with silver impregnation methods. J Comp Neurol 1965;124:71–99.

O'Dwyer NJ, Ada L, Neilson PD. Spasticity and muscle contracture following stroke. Brain 1996;119:1737–49.

Patrick E, Ada L. The Tardieu scale differentiates contracture from spasticity whereas the Ashworth scale is confounded by it. Clin Rehabil 2006;20:173–82.

Powers RK, Marder-Meyer J, Rymer WZ. Quantitative relations between hypertonia and stretch reflex threshold in spastic hemiparesis. Ann Neurol 1988;23:115–24.

Rho MJ, Cabana T, Drew T. Organization of the projections from the pericruciate cortex to the pontomedullary reticular formation of the cat: a quantitative retrograde tracing study. J Comp Neurol 1997;388:228–49.

Rosengren SM, McAngus Todd NP, Colebatch JG. Vestibular-evoked extraocular potentials produced by stimulation with bone-conducted sound. Clin Neurophysiol 2005;116:1938–48.

Rosengren SM, Welgampola MS, Colebatch JG. Vestibular evoked myogenic potentials: past, present and future. Clin Neurophysiol 2010;121:636–51.

Rosengren SM, Govender S, Colebatch JG. Ocular and cervical vestibular evoked myogenic potentials produced by air- and bone-conducted stimuli: comparative properties and effects of age. Clin Neurophysiol 2011;122:2282–9.

Schepens B, Drew T. Descending signals from the pontomedullary reticular formation are bilateral, asymmetric, and gated during reaching movements in the cat. J Neurophysiol 2006;96:2229–52.

Sharpe JA, Lo AW. Voluntary and visual control of the vestibuloocular reflex after cerebral hemidecortication. Ann Neurol 1981;10:164–72.

Sheean G. Neurophysiology of spasticity. In: Barnes MP, Johnson GR, editors. Upper motor neurone syndrome and spasticity: clinical management and neurophysiology. Cambridge: Cambridge University Press; 2001. p. 12–78.

Sherrington CS. Decerebrate rigidity, and reflex coordination of movements. J Physiol 1898;22:319–32.

Singer OC, Humpich MC, Laufs H, Lanfermann H, Steinmetz H, Neumann-Haefelin T. Conjugate eye deviation in acute stroke: incidence, hemispheric asymmetry, and lesion pattern. Stroke 2006;37:2726–32.

Teasell R, Bayona NA, Bitensky J. Plasticity and reorganization of the brain post stroke. Top Stroke Rehabil 2005;12:11–26.

Tijssen CC, van Gisbergen JA, Schulte BP. Conjugate eye deviation: side, site, and size of the hemispheric lesion. Neurology 1991;41:846–50.

Todd NP, Rosengren SM, Aw ST, Colebatch JG. Ocular vestibular evoked myogenic potentials (OVEMPs) produced by air- and bone-conducted sound. Clin Neurophysiol 2007;118:381–90.

Urban PP, Wolf T, Uebele M, Marx JJ, Vogt T, Stoeter P, et al. Occurence and clinical predictors of spasticity after ischemic stroke. Stroke 2010;41:2016–20.
Watkins CL, Leathley MJ, Gregson JM, Moore AP, Smith TL, Sharma AK. Prevalence of spasticity post stroke. Clin Rehabil 2002;16:515–22.
Weber KP, Rosengren SM, Michels R, Sturm V, Straumann D, Landau K. Single motor unit activity in human extraocular muscles during the vestibulo-ocular reflex. J Physiol 2012;590:3091–101.
Welgampola MS, Migliaccio AA, Myrie OA, Minor LB, Carey JP. The human sound-evoked vestibulo-ocular reflex and its electromyographic correlate. Clin Neurophysiol 2009;120:158–66.
Wicke W, Wasicky R, Brugger PC, Kaminski S, Lukas JR. Histochemical and immunohistochemical study on muscle fibers in human extraocular muscle spindles. Exp Eye Res 2007;84:670–9.
Wilson LR, Gandevia SC, Inglis JT, Gracies J, Burke D. Muscle spindle activity in the affected upper limb after a unilateral stroke. Brain 1999;122:2079–88.
Wilson VJ, Peterson BW. Vestibulospinal and reticulospinal systems. In: Comprehensive physiology. Supplement 2: handbook of physiology, the nervous system, motor control, 2011. p. 667–702. http://dx.doi.org/10.1002/cphy.cp010214. First published in print 1981.
Wissel J, Manack A, Brainin M. Toward an epidemiology of poststroke spasticity. Neurology 2013;80:S9–S13.
Wright J, Rang M. The spastic mouse. And the search for an animal model of spasticity in human beings. Clin Orthop Relat Res 1990;253:12–9.
Young RR. Spasticity: a review. Neurology 1994;44:S12–20.